

Numerical study of surface waves generated by low frequency EM field for silicon refinement

V. Geza¹, J. Vencels¹, G. Zageris¹ and S. Pavlovs¹

¹ University of Latvia, LV-1002, Riga, Latvia

Corresponding author: vadims.geza@lu.lv.

Abstract

One of the most perspective methods to produce solar grade silicon is refinement via metallurgical route. The most critical part of this route is refinement from boron and phosphorus due to high segregation coefficients. One possible approach to remove boron is use of reactive gas on surface of silicon melt. An approach of creating surface waves on silicon melt's surface is proposed in order to enlarge its area and accelerate removal of boron via chemical reactions.

This paper focuses on numerical analysis of surface wave creation by means of low frequency magnetic field. Frequency of magnetic field and its amplitude significantly change the character of surface waves with most changes occurring when waves become nonlinear. Mechanism of impurity removal from silicon surface to the gaseous phase is directly connected with surface area enlargement. It was found that two effects are responsible for enhancement of refinement rate – enlargement of surface area and wave-assisted diffusion close to the surface of silicon.

Keywords : silicon refinement, surface waves, electromagnetic stirring

Introduction

The exhaustion of fossil fuel resources, global warming, and increased energy consumption all make finding alternative energy sources important. In terms of environmental impact, solar energy is one of the most perspective and attractive sources. However, development of solar power is limited by the solar power costs in comparison to other power sources. As shown in [1], by 2020 the energy cost for solar power is still expected to be higher than for hydro, onshore wind, geothermal, nuclear and even biomass energy sources. Reduction of solar cell production costs is necessary for this technology to develop, and one solution is to reduce the cost of raw materials like polysilicon. Solar cell costs are directly linked to polysilicon production costs, which can be reduced by lowering energy consumption during solar grade silicon (SoG-Si) production.

In many investigations phosphorus removal is found to be the most challenging task, since the purity threshold (< 1 ppm) was not reached [2]. Although, oxidation and slag refinement is simple process for removing phosphorus from silicon, it is insufficient to reach low purity threshold. Mostly used approach for phosphorus removal is evacuation, it is dependent on free surface area and bulk melt stirring. Refinement enhancement can be achieved by superposing DC and AC magnetic fields [3]. Furthermore, this impact creates also mixing effect in the bulk melt, which is also important for boron removal. In comparison, classical induction stirring can enhance only bulk melt mixing, leaving surface area size unchanged.

Known approach for boron removal is blowing of oxidizing gas on free surface [4], and with additional creation of surface waves by means of electromagnetic impact thus creating capillary waves and increasing surface area. Previously mentioned electromagnetic impact technology (superposition of DC and AC fields) can be used for boron evaporation, because it enhances surface area and stirring.

Highest boron refining rates can be achieved with plasma refining, but it has high energy demand. In reactive gas refining, concentration of boron changes according to first order rate law

$$\ln \left[\frac{C_{B,0}}{C_{B,t}} \right] = k_B \frac{A}{V} t \quad (1)$$

Here C_B – boron concentration with indices after comma indicating time, A is the area of interfacial surface between oxidizing gas and silicon melt, V is the volume of silicon melt, t is time, k_B is boron mass transfer coefficient at the surface, measured in $\mu\text{m/s}$. k_B is determined experimentally and is dependent on oxidizing gas supply rate, type of oxidizing gas and melt temperature. Creation of surface waves would increase A/V ratio, thus speeding up boron removal. Typical k_B values found in literature are 6 – 40 $\mu\text{m/s}$, and k_P are 2-5 $\mu\text{m/s}$ for phosphorus.

Modelling of free surface waves

A 3D problem of mercury with free surface is considered. The mercury tank is surrounded by inductor, which creates alternating magnetic field, see Fig. 1 (a) for illustration. A similar device and experiment was described in [5]. This mercury experiment is only used for model validation purposes.

In this model, mercury properties were set in the melt domain – electrical conductivity $\sigma_{\text{melt}}=1.04 \cdot 10^6$ S/m, kinematic



viscosity $\nu_{\text{melt}} = 1.14 \cdot 10^{-7} \text{ m}^2/\text{s}$, density $\rho = 13534 \text{ kg/m}^3$, surface tension $\gamma = 0.5 \text{ N/m}$ and contact angle $\theta = 90^\circ$. The inductor has homogeneous current distribution with density $J_{\text{ampl}} = 6.5 \cdot 10^6 \text{ A/m}^2$ and frequency $f = 14 \text{ Hz}$. Turbulence model $k-\epsilon$ is used, and maximal Courant number is set to 0.4. The transient simulation reached flow time 4 sec.

For numerical simulations we use two open-source software packages – the finite element multi-physics simulation code Elmer and computational fluid dynamics code OpenFOAM. Efficient parallel coupling between both codes is done using EOF-Library [6].

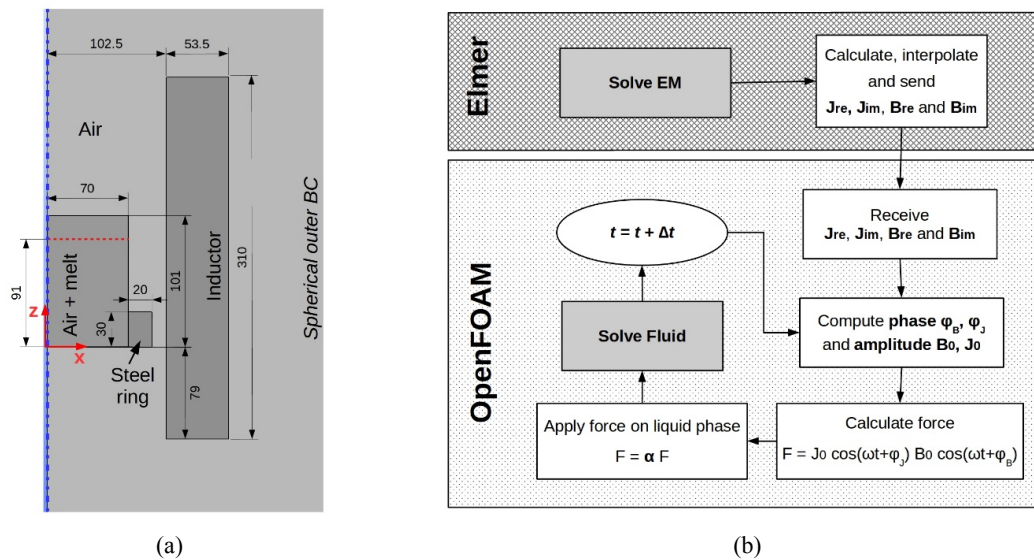


Fig. 1: (a) Schematic drawing for 2D axisymmetric model, where vertical dashed line is symmetry axis and horizontal dashed line is melt's initial filling level. (b) Computational scheme for coupled OpenFOAM and Elmer simulation

Computation scheme is shown in Fig. 1 (b). OpenFOAM package solves electromagnetic quantities in Elmer package and fluid dynamics with free surface using volume of fluid (VOF) method in OpenFOAM. Elmer solves the complex problem for the time-harmonic electromagnetic (EM) field, then J and B amplitudes and the corresponding phases are computed. Here electromagnetic field is not recalculated when free surface is changed. This effect is neglected to speed up the simulation time. This approach can be used because penetration depth of EM field is much larger than free surface wave amplitude.

Results of 3D surface simulation show different wave structure depending on the strength of magnetic field. Three different regimes were obtained (see Fig. 2):

- Regular axisymmetric waves. Wave structure similar to Fig. 2 (upper-left), but without azimuthal waves. This is most regular pattern and is obtained at weak magnetic field values (below 0.15 T).
- Regular axisymmetric waves with azimuthal waves, seen in Fig. 2 (upper-left and bottom-left). This regime is obtained at stronger magnetic fields (0.15-0.21 T)
- Azimuthal waves Fig. 2 (upper-right). Here axisymmetric have disappeared. This regime appears at magnetic fields above 0.21 T.

These results are in agreement with findings of Galpin and Fautrelle [35]. However, they found fourth regime, highly chaotic surface motion with jets of liquid metal appearing on the surface. This regime appears at even higher magnetic field values. In this research, such magnetic field values were never used.

For refinement of silicon, important parameter is surface area enlargement $S(t)/S(0)$. Here $S(t)$ is surface area at some time, but $S(0)$ is area of surface at rest. Fig. 2 (bottom-right) shows surface enlargement for different magnetic field values. For lowest magnetic field strength, $B=0.18 \text{ T}$, the area enlargement is slightly above 1%, for $B=0.21 \text{ T}$ – about 2.5%, for $B=0.25 \text{ T}$ – about 4.5%.

Modelling of silicon refining process

For silicon refinement, a system consisting of gas domain with incoming jet (see scheme in Fig. 3) and molten silicon domain is modelled. The computations of silicon melt flow in crucible and gas flow injected with lance are performed using ANSYS FLUENT package with $k-\epsilon$ turbulence model. Boron concentration both in melt and in gas is traced with UDS (User Defined Scalar) option in ANSYS FLUENT. Lorentz force, induced by coil is modelled with EMAG module

of ANSYS Multiphysics package. Parameters of simulations are following:

- radius of crucible with silicon melt is 0.031 m;
- argon jet lance diameter is 0.0062 m;
- argon flow rate is 4 l_N/min ;
- boron-carrying-molecule diffusivity in argon is $3.4 \cdot 10^{-4} m^2/s$;
- boron diffusivity in silicon is $2.4 \cdot 10^{-8} m^2/s$;
- amplitude value of electrical current in coil is 10 kA.

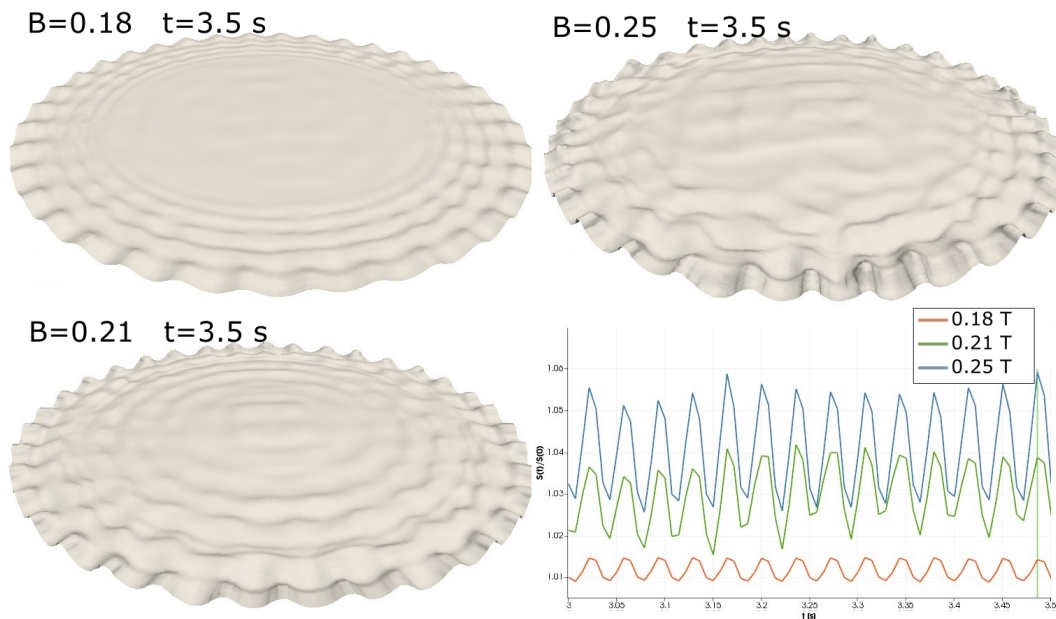


Fig. 2: Free surface shape after 3.49 seconds for different magnetic field strength values and corresponding surface area enlargement (bottom right)

In reality there is a chemical reaction taking action on the surface, where reacting gas oxidizes boron and new molecules are formed which carry boron away from the melt. In this simulation idealized system is used, where one scalar variable was used in both melt and gas domain. In the beginning, fixed concentration of boron in melt is assumed. Then, gas with boron concentration 0 is blown on the surface of silicon, and part of boron is removed.

This simulation was done to estimate the boron mass transfer coefficient k_B at gas–silicon interface (see equation 1). The mean boron concentration in melt during this refinement process simulation is shown in Fig 4. The estimated k_B value based on simulation of 5 hours of refinement is $12.7 \mu m/s$. This value is in good agreement with measurement results in [4].

To account the influence of surface waves, a simulation with only gas domain was performed. Gas domain had moving bottom boundary – harmonic wave motion was assigned to it. To measure the influence of different wave amplitudes and frequencies, a boron flux through outlet was observed.

Surface waves with realistic amplitudes did not show any enhancement in boron flux in comparison to static gas–silicon interface. The reason for that is strong diffusion, which leads to diffusion length scale comparable to wave amplitude. It turned out that refinement enhancement can be observed only if following criterion is met:

$$A > 4 \sqrt{\frac{D}{f}}$$

Here A – wave amplitude, D – diffusion coefficient of boron-carrying molecule in gas, f – frequency of waves. Wave amplitude in this criterion is, however, linked to frequency, therefore it cannot be directly used to estimate required frequency.

Boron flux through outlet of the gas domain was obtained in simulations with different wave amplitudes (Fig. 5). There is obvious increase of boron flux with increase of amplitude. However, values normalized on surface area lay on the horizontal line, matching values for flux with static surface. This clearly indicates that boron flux increase is connected

with surface area enlargement.

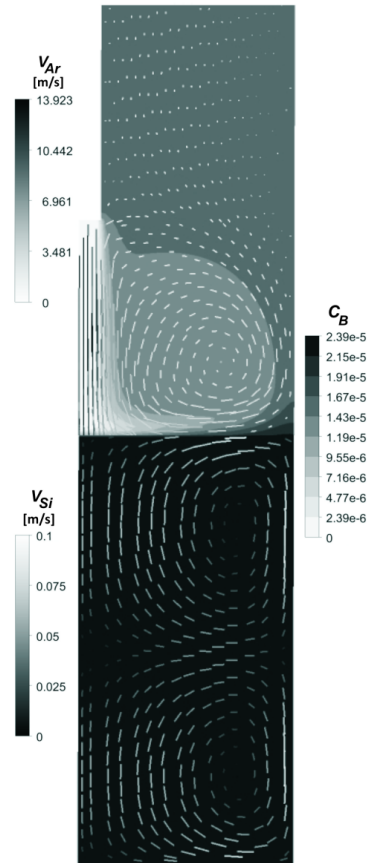


Fig. 3: Modelling of boron removal from silicon with oxidizing gas jet: C_B – boron concentration, v_{Si} and v_{Ar} – silicon melt flow and argon flow velocities for $t = 0.41 h$

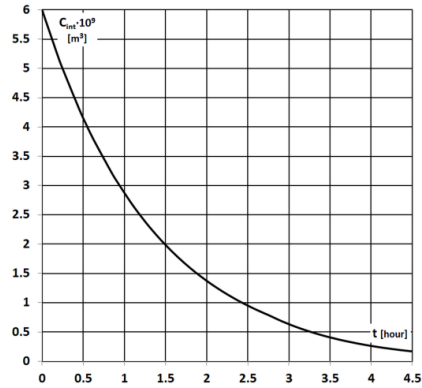


Fig. 4: Boron integral concentration C_{int} in silicon melt as function of silicon refining process time t

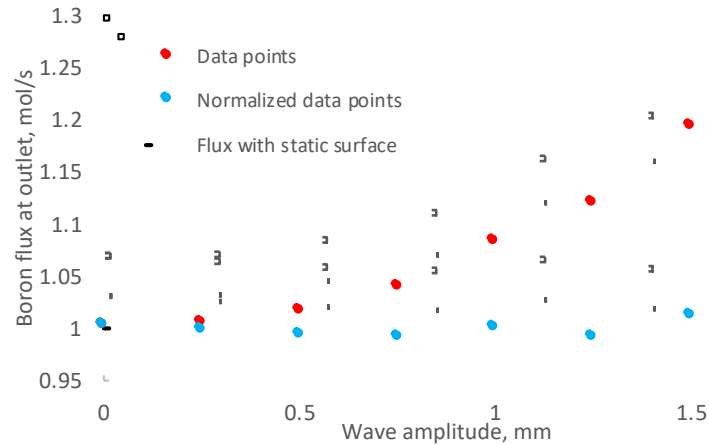


Fig 5: Integral boron flux through outlet dependence on wave amplitude. Error bars – 4% of the value. Data are obtained when steady state is reached

Conclusions

Surface waves on liquid metal surface can be captured using VOF approach. Simulations showed three wave regimes, with less structured waves appearing at higher magnetic field values. Increase of magnetic field amplitude also leads to increased surface area, which is important for refinement. Simulations show clear dependence of refinement rate on surface area.

Acknowledgment

This work was funded by European Regional Development Fund under contract “Refinement of metallurgical grade silicon using smart refinement technologies” (No. 1.1.1.1/16/A/097).

References

1. U.S. Energy Information Administration (EIA) – Source // www.eia.gov (retrieved 2016-06-07)
2. Khattak C P, Joyce D B, Schmidt F 2002 Solar Energy Materials and Solar Cells 74 77
3. Bojarevičs A, Beinerts T, Grants I, Kaldre I, Šivars A, Gerbeth G, Gelfgat Yu 2015 Magnetohydrodynamics 51 437
4. Sortland Ø S, Tangstad M 2014 Metallurgical and Materials Transactions E 1 211

5. Saadi B, Bojarevics A, Fautrelle Y, Etay J 2005 Récents Progrès en Génie des Procédés, Numéro 92 (Paris)
6. Vencels J, Jakovics A, Geza V, Scepanskis M 2017 XVIII Int. UIE-Congress (Hannover) p 312